

Hibbingite, $\gamma\text{-Fe}_2(\text{OH})_3\text{Cl}$, a new mineral from the Duluth Complex, Minnesota, with implications for the oxidation of Fe-bearing compounds and the transport of metals

BERNHARDT SAINI-EIDUKAT*

Institut für Geowissenschaften, Montanuniversität, A-8700 Leoben, Austria

HENRYK KUCHA

Institute of Geology and Mineral Deposits, Academy of Mining and Metallurgy,
aleja Mickiewicza 30, 30-059 Kraków, Poland

HANS KEPPLER

Bayerisches Geoinstitut, Universität Bayreuth, Postfach 10 12 51, 95440 Bayreuth, Germany

ABSTRACT

Hibbingite is a new divalent iron hydroxychloride in the atacamite family from the Duluth Complex, Minnesota. It occurs as vein fillings in drill core of partially serpentinized, troctolitic rocks. It is associated with serpentine, olivine, plagioclase, biotite, and secondary magnetite or goethite. Grain sizes can be up to 700 μm long and 100 μm wide.

Electron microprobe analysis yielded an empirical formula (based on $\text{O} + \text{Cl} = 4$ and OH by difference) of $(\text{Fe}_{1.72}\text{Mg}_{0.21}\text{Mn}_{0.06}\text{Si}_{0.01})_{\Sigma 2.00}(\text{OH})_{3.00}[\text{Cl}_{0.87}(\text{OH})_{0.12}]_{\Sigma 0.99}$. The simplified formula is $\gamma\text{-Fe}_2(\text{OH})_3\text{Cl}$. Its d_{calc} is 3.04 g/cm^3 ; it is soluble in H_2O and ethanol. The mineral is slightly pleochroic and colorless to pale green when unoxidized but becomes increasingly reddish with oxidation. It may manifest a parting or cleavage perpendicular to vein walls. The approximate index of refraction is 1.6–1.7. It has first-order gray birefringence and is length-fast with parallel extinction. In reflected light, birefractance is observable under crossed polars. Fresh samples show greenish internal reflections, which become reddish with oxidation. The IR spectrum shows a strong peak at 3552 cm^{-1} due to the OH^- stretching vibration. The crystal field band of Fe^{2+} occurs at 12550 cm^{-1} . Oxidized samples show a $\text{Fe}^{2+} \rightarrow \text{Fe}^{3+}$ intervalence charge transfer band at about 20000 cm^{-1} .

Electron diffraction data agree with X-ray diffraction data of similar, unnamed specimens from the literature. The d_{obs} (hkl) of some electron diffraction lines, in ångströms, are 7.08 (001), 5.68 (011), 5.07 (110), 4.60 (020), 4.20 (111), 3.70 (120), 3.55 (002), 2.93 (112), 2.37 (202), 2.30 (040), 2.14 (113), 1.90 (203), 1.65 (242). The data were indexed on an orthorhombic unit cell by analogy with $\beta\text{-Mg}_2(\text{OH})_3\text{Cl}$, giving $a = 6.31(6)$, $b = 9.20(4)$, $c = 7.10(7)$ Å, $V = 412.17$ Å³, and $Z = 4$. The probable space group is $Pnam$, which is also by analogy with atacamite-type compounds.

The occurrence of hibbingite has implications for serpentinization processes, sea-floor alteration by hydrothermal fluids, and metal transport in Cl-bearing solutions. In the Duluth Complex, it probably formed as a result of Cl-rich fluids participating in serpentinization reactions. It may be a previously unrecognized intermediate phase during such processes as the corrosion of steel in brines and the terrestrial weathering of meteorites.

Hibbingite is named after the city of Hibbing, Minnesota, and type material is preserved in the Drill Core Library of the Department of Natural Resources, Hibbing, Minnesota.

INTRODUCTION

Whereas orthorhombic nickel, manganese, and magnesium hydroxyhalogenides have been synthesized (Oswald and Feitknecht, 1963), the only known natural analogues are kempite and atacamite; botallackite is monoclinic, and paratacamite is hexagonal. This paper

describes a newly discovered naturally occurring orthorhombic iron hydroxychloride, hibbingite.

Hibbingite and its polymorphs have been identified in partially serpentinized troctolites from the Duluth Complex, Minnesota (Dahlberg and Saini-Eidukat, 1991), in sulfide ore from the Sudbury Complex, Canada (Springer, 1989), and the Noril'sk intrusion, Russia (Rudashevsky, 1992 personal communication), and in terrestrially weathered meteorites (Buchwald, 1989).

The mineral was first recognized from investigations of

* Present address: Department of Geosciences, North Dakota State University, Fargo, North Dakota 58105, U.S.A.

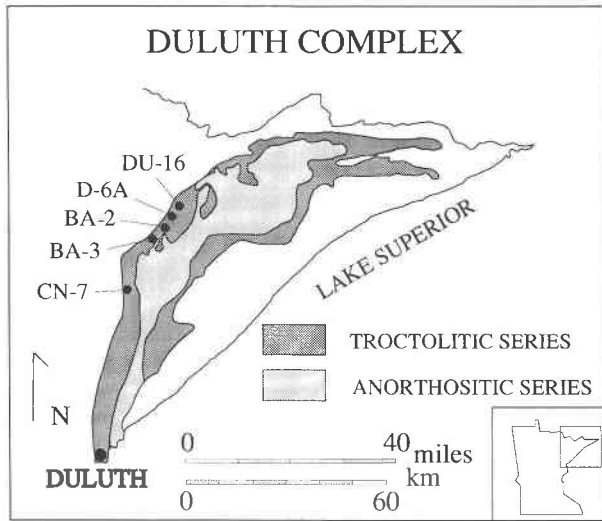


Fig. 1. Generalized map of the Duluth Complex showing locations of drill cores in which hibbingite has been found. The inset shows a map of Minnesota with a location box.

its alteration product, akaganéite, found on the surfaces of drill cores stored in humid environments. The alteration forms reddish encrustations on the drill-core surfaces and is Cl-rich (Dahlberg and Saini-Eidukat, 1991). Thin sections made from these encrusted drill cores revealed the presence of an Fe- and Cl-rich mineral.

Hibbingite is named for the city of Hibbing, Minnesota. Type material is preserved and catalogued by drill-core numbers in the Drill Core Library of the Department of Natural Resources, Hibbing, Minnesota. Hibbingite has been approved by the IMA Commission on New Minerals and Mineral Names.

OCCURRENCE AND APPEARANCE

Hibbingite occurs in drill core of partially serpentinized troctolitic or peridotitic rocks from near the base of the

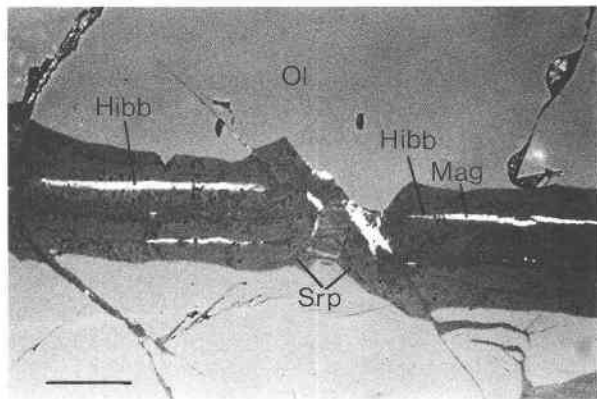


Fig. 2. Photomicrograph of hibbingite (Hibb) and a magnetite (Mag) pseudomorph after hibbingite, both enclosed in the serpentinite (Srp) alteration of olivine (Ol). Scale bar = 40 μm .

TABLE 1. Drill-core numbers and depth intervals (m) in which hibbingite has been identified microscopically

DU-16	D-6A	BA-2	BA-3	CN-7
1082.0	442.8–	1020.2	718.1–	262.0
1082.8	443.5	1024.0	718.4	
1083.0				
1084.8	559.9–		793.5–	
1096.2	560.5		794.0	

Duluth Complex, Minnesota (Fig. 1, Table 1). It occurs most often as vein fillings in close textural association with serpentinite and may exhibit feathery intergrowth textures with serpentine minerals. Grain sizes vary from approximately 20 to 700 μm long and from approximately 3 to 100 μm wide. Veins of hibbingite also may crosscut olivine or plagioclase grains or occur along cleavage planes of biotite or in grain boundaries between these materials. Often it is lens-shaped, especially in biotite. Magnetite, maghemite, and goethite are normally found as micrometer-sized inclusions in hibbingite and are apparently alteration products from it. The abundant secondary vein-filling magnetite in samples in which the Fe- and Cl-bearing mineral has not been found appear pseudomorphic after hibbingite (Fig. 2).

In transmitted light (Fig. 3), hibbingite is slightly pleochroic and colorless to pale green in its unoxidized form but increasingly yellow-red with oxidation. A distinct parting or cleavage perpendicular to the vein walls in some cases manifests itself as a platy habit. Its approximate index of refraction, estimated from Becke tests vs. olivine, serpentine, and plagioclase, is 1.6–1.7. Its birefringence is first-order gray, and it is length-fast, with parallel or nearly parallel extinction. In reflected light, bireflectance is observable under crossed polars. Freshly polished, unoxidized samples show greenish internal reflections, which become red with oxidation. The polished surface may display a pitted nature, which could be due either to the effects of polishing or to the natural porosity of the mineral. This texture is often preserved in the magnetite or goethite pseudomorphs.

A distinctive feature seen in reflected light is the formation of hydration bubbles on the mineral surface after it has been exposed to atmospheric moisture; these bubbles may crystallize as salts on the thin section. After days or weeks hibbingite may disappear completely from the thin section. Because it is soluble in H_2O and ethanol, all polished or thin sections were made using Rehwald lead-lap polishing equipment and oil.

CRYSTALLOGRAPHIC DATA

Two attempts were made to obtain an X-ray diffraction pattern of hibbingite in thin section using a Rigaku micro-X-ray diffractometer (beam diameter 20 μm), fitted with a three-axis sample oscillation mechanism and a fixed, curved, position-sensitive counter. Although several peaks were detected that are consistent with the proposed structure and d values obtained by Springer (1989) and our electron diffraction values, neither attempt pro-

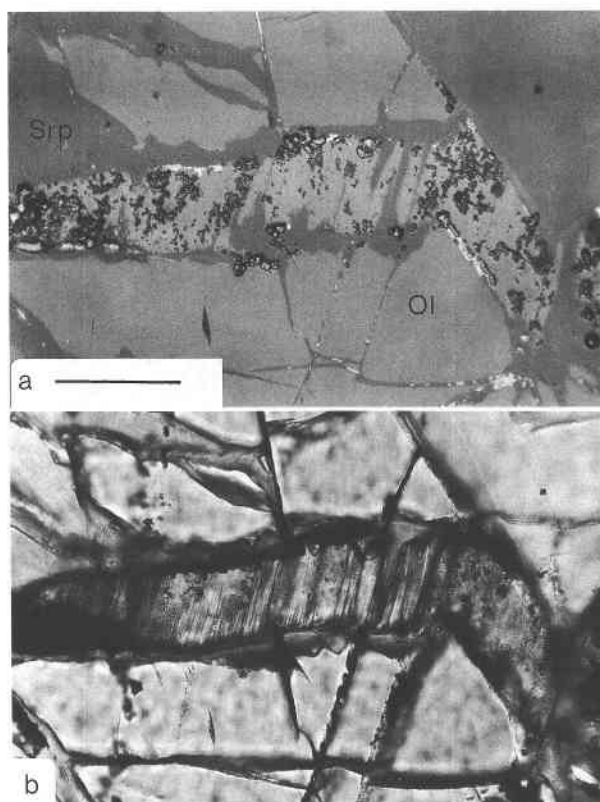


Fig. 3. Photomicrographs of hibbingite in the serpentine (Srp) alteration from olivine (Ol), from drill core DU-16, 1082.8 m. Scale bar = 50 μm . (a) Reflected light, showing surface pitting and the hydration products. (b) Transmitted, plane-polarized light.

duced enough peaks for an unambiguous identification. We believe this is because of the strong preferred orientation of the crystals in the sample, leading to insufficient randomization by the diffractometer's oscillators.

An electron diffraction study of hibbingite (Fig. 4) was made using a JEOL 100C transmission electron microscope at 100-kV accelerating voltage (Academy of Mining and Metallurgy, Kraków). A description of the study techniques was presented in Kucha et al. (1993). Particles for the TEM study were collected under an optical microscope from areas previously analyzed by electron microprobe. The standard used was gold, either separate and to the side of the hibbingite or as a support film on the specimen grid. In the first case, the precision of the measurement of d values is $\pm 1\%$ of the measured value, and in the second case, the precision is $\pm 0.05\%$ of the measured value.

The electron diffraction data cannot be used to assign unequivocally a symmetry and space group to hibbingite; however, two lines of argument can be used to support the inferences presented below. First, crystallographic data from electron diffraction are compared with those calculated from X-ray diffraction data for $\text{Fe}_2(\text{OH})_3\text{Cl}$ from the Strathcona mine measured by Springer (1989). Sec-

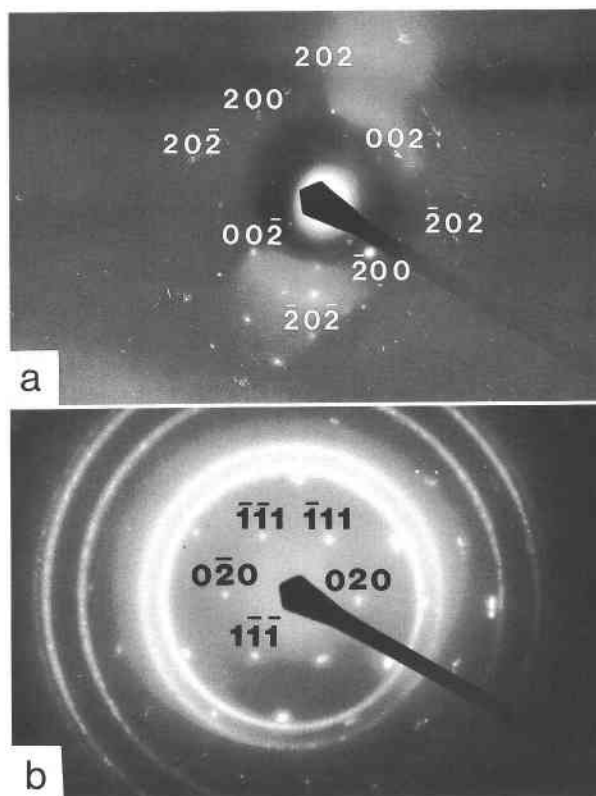


Fig. 4. Single-crystal electron diffraction patterns of hibbingite: (a) [010] zone axis and (b) [101] zone axis.

ond, our data are compared with data from other minerals and compounds of the atacamite type.

In Table 2, measured d values and indexed lines obtained by electron diffraction are compared with d values calculated on the basis of our measured lattice constants, and are in excellent agreement with d values for $\text{Fe}_2(\text{OH})_3\text{Cl}$ measured by Springer (1989) using X-ray diffraction. In Table 3, the crystallographic data of hibbingite from the Duluth Complex are compared with minerals and compounds of the atacamite type. From these data, we infer a space group of $Pnam$ for hibbingite and calculate a density of 3.04 g/cm^3 . Table 3 compares the cell parameters of $\beta\text{-Mg}_2(\text{OH})_3\text{Cl}$, $\text{Fe}_2(\text{OH})_3\text{Cl}$ from the Strathcona mine (calculated from the X-ray diffraction data in Springer, 1989), and hibbingite from the Duluth Complex. Table 3 also compares axial ratios of hibbingite with other orthorhombic hydroxyhalogenides of divalent metals. All these comparisons support our interpretation made from the electron diffraction data, namely that (1) $\text{Fe}_2(\text{OH})_3\text{Cl}$ from the Strathcona mine is the same mineral as hibbingite from the Duluth Complex, and (2) hibbingite is isostructural with the atacamite group of minerals.

CHEMICAL DATA

Hibbingite grains in thin section from drill cores D-6A (560.0 m) and BA-3 (718.12 m) were analyzed by elec-

TABLE 2. Comparison of electron diffraction data from hibbingite with X-ray data from $\text{Fe}_2(\text{OH})_3\text{Cl}$

No.	Strathcona*		hkl	Hibbingite**	
	l/l_0	d		d_{meas}	d_{calc}
1			001†	7.08	7.10
2	4	5.62	011	5.68	5.63
3	2	5.16	110	5.07	5.20
4			(101)†	4.70	4.72
5	0.5	4.63	020	4.60	4.60
6	1	4.17	111	4.20	4.20
7			021	3.89	3.86
8			120	3.70	3.72
9			002	3.55	3.55
10			121	3.26	3.29
11			(102)†	3.10	3.09
12	6	2.86	112	2.93	2.93
13			201	2.89	2.88
14	0.5	2.585	220	2.60	2.60
15			131	2.60	2.57
16			221	2.45	2.44
17	10	2.33	202	2.37	2.36
18	1	2.28	040	2.30	2.30
19			(103)†	2.20	2.22
20	1	2.185	140	2.17	2.16
21	5	2.12	113	2.14	2.15
22	1	2.05	222	2.08	2.10
23	2	1.87	203	1.90	1.89
24	1	1.80	241	1.80	1.80
25	2	1.745	004, 312	1.77	1.77
26	5	1.652	242	1.65	1.65
27	1	1.597	233, 143	1.60	1.61
28	0.5	1.453	224	1.45	1.47
29	1	1.406	044	1.40	1.405
30			171	1.270	1.266

Note: missing rows in the Strathcona data that appear in the TEM data for hibbingite agree with indexed lines for $\beta\text{-Mg}_2(\text{OH})_3\text{Cl}$ (PDF 12-410).

* X-ray diffraction data from Springer (1989).

** Electron diffraction data from this study.

† May occur by double diffraction.

TABLE 4. Chemical composition of hibbingite, as measured by electron microprobe, compared with data from Springer (1989) and the theoretical formula

	This study* (sd)	Strathcona**	Theoretical formula
	Weight percent		
Fe	49.02(1.29)	53.90	56.36
Mn	1.49(0.28)	n.a.	
Mg	2.62(0.37)	n.a.	
Si	0.10(0.08)	n.a.	
Cl	17.39(1.13)	18.20	17.89
OH†	29.92(1.90)	27.90	25.75
Total	100.56	100.00	100.00
Atoms			
Fe	1.76	1.93	2.00
Mn	0.05	n.a.	
Mg	0.22	n.a.	
Si	0.01	n.a.	
Cl	0.98	1.03	1.00
OH	3.52†	3.28†	3.00

Note: analyses were performed on an ARL-SEM-Q (University of Graz) using Bence-Albee correction factors. Standards used were atacamite (Cl), kaersutite (Fe, Al, Si), tephroite (Mn), and olivine (Mg). The analyzing conditions were 15-kV accelerating voltage and 20-nA sample current, as measured on brass; n.a. = not analyzed.

* Average of eight analyses from samples 90917-12-6 (DDH D-6A, 660 m) and 90917-17-2 (DDH BA-3, 718 m). Analysis includes Al < 0.05 wt% and Cr < 0.05 wt%.

** From Springer (1989).

† By difference.

tron microprobe (Table 4). These data supersede the preliminary data given in Dahlberg and Saini-Eidukat (1991). Although care was taken to measure at positions away from serpentinite, the small amounts of Si measured may be due to small silicate grains associated with the hibbingite.

Fe valence

Fe valence was determined using two methods. In the first, X-ray emission spectroscopy was employed (Albee and Chodos, 1970). The $\text{FeL}\beta/\text{L}\alpha$ ratio of X-ray emission

peaks was measured using a Cameca Camebax microprobe at the Academy of Mining and Metallurgy (Kraków) with a TAP crystal. Standards used were magnetite, wüstite, and hematite, the beam size was 7 μm , and the analyzing conditions were 15-kV accelerating voltage and 200-nA sample current, measured on Fe metal. These conditions resulted in a count rate of approximately 1000 counts/s on Fe metal. $\text{FeL}\beta$ and $\text{FeL}\alpha$ were each measured using a 50-step peak search (dwell time was 20 s), after which peak position and height were calculated using least-squares root fitting. The precision of the ratio measurement is 5–6% of the measured value. The ratio was checked by moving the spectrometer to the calculated peak positions and counting the $\text{FeL}\alpha$ and $\text{FeL}\beta$ intensities for 30 s. If the two ratio measurements agreed, then the measurement was accepted. As seen in Figure 5, less oxidized grains exhibiting greenish internal reflections have higher $\text{FeL}\beta/\text{L}\alpha$ ratios than more oxidized

TABLE 3. Unit-cell data from hibbingite [$\gamma\text{-Fe}_2(\text{OH})_3\text{Cl}$] from the Duluth Complex compared with data from minerals and compounds of the atacamite type*

Substance	Unit-cell parameters (Å)			Axial ratio a:b:c	V (Å ³)	V/ $\text{Me}_2(\text{OH})_3\text{X}$ (Å ³)	Source
	a	b	c				
$\gamma\text{-Fe}_2(\text{OH})_3\text{Cl}$ (hibbingite)**	6.31(6)	9.20(4)	7.10(7)	0.686:1:0.772	412.2	103.1	this study
$\text{Fe}_2(\text{OH})_3\text{Cl}$ (Strathcona)	6.26	9.19	6.98	0.681:1:0.760	401.6	100.4	1
$\delta\text{-Cu}_2(\text{OH})_3\text{Cl}$ (atacamite)	6.01	9.13	6.84	0.658:1:0.749	375.3	93.8	2
$\beta\text{-Mn}_2(\text{OH})_3\text{Cl}$ (kempite)	6.47	9.52	7.12	0.679:1:0.747	438.5	109.6	3
$\beta\text{-Mg}_2(\text{OH})_3\text{Cl}$	6.24	9.19	6.87	0.680:1:0.739	393.0	98.3	PDF 12-410
$\beta\text{-Ni}_2(\text{OH})_3\text{Cl}$	6.18	9.07	6.71	0.681:1:0.740	375.9	94.0	3
$\text{Mn}_2(\text{OH})_3\text{Br}$	6.56	9.66	7.23	0.679:1:0.750	458.2	114.6	3

Note: 1 = Springer (1989), 2 = Palache et al. (1951), 3 = Oswald and Feitknecht.

* All orthorhombic, $Pnam$, $Z = 4$, except where noted otherwise.

** Space-group inferred.

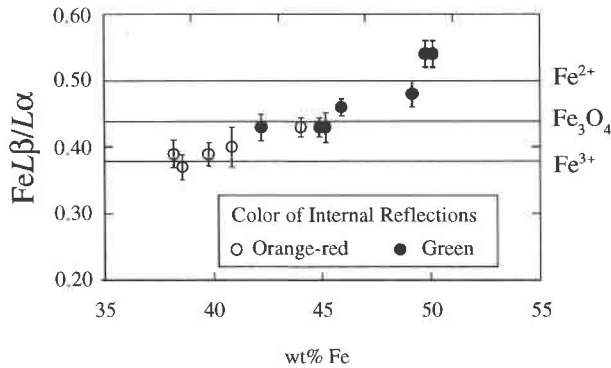


Fig. 5. $FeL\beta/L\alpha$ plotted against wt% Fe for hibbingite from the Duluth Complex. The horizontal lines indicate measured values of the $FeL\beta/L\alpha$ ratio on the standards wüstite (Fe^{2+}), magnetite (Fe_3O_4), and hematite (Fe^{3+}).

grains exhibiting reddish internal reflections. These data indicate that Fe in hibbingite is divalent.

The second method used was visible-light absorption spectroscopy. The samples, polished thin sections 30 μm thick, were mounted on glass with epoxy, prepared using diamond grit and oil on lead laps, and coated with oil and a cover glass to retard oxidation. Prior to measurement, the cover glass was removed, and the oil was cleaned from the surface with heptane. The measurements were made on a Bruker IFS 120 HR FTIR spectrometer equipped with a Bruker A590 IR microscope at the Bayerisches Geoinstitut, Bayreuth. Two samples were measured, one from drill hole D-6A, at 560.0 m and another from drill hole DU-16, at 1084.8 m. The spot size of the beam was between 25 and 40 μm . Background was collected on thin-section glass.

Figure 6 shows two visible-light absorption spectra for hibbingite in sample DU-16, at 1084.8 m. The lower spectrum is for a relatively unoxidized (clear) grain and shows a peak centered at 12550 cm^{-1} , which indicates the presence of Fe^{2+} (e.g., Rossman, 1988). This band corresponds to the transition ${}^5T_{2g} \rightarrow {}^5E_g$ of Fe^{2+} in an octahedral site. No obvious signs of Jahn-Teller splitting are seen, but they might be difficult to detect because of the broadness of the band. The top spectrum is from a nearby oxidized grain (reddish in color), which shows a band possibly due to $Fe^{2+} \rightarrow Fe^{3+}$ intervalence charge transfer near 20000 cm^{-1} . The position of this band is very similar to the intervalence charge transfer band in synthetic garnet ($Fe_3^{2+}Fe_3^{3+}Si_3O_{12}$; Khomenko et al., 1993). The continuous increase of absorbance with wavenumber seen in both spectra is caused by diffusive scattering due to imperfections of the crystal. These data confirm our conclusions on the basis of X-ray spectroscopy and strongly support the idea of the predominance of divalent Fe in hibbingite.

The OH ion

The presence or absence of OH in hibbingite was investigated using two methods. In the first, X-ray emission

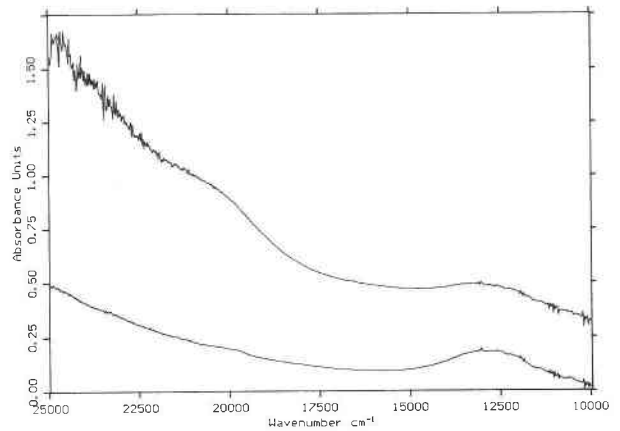


Fig. 6. Two visible-light absorption spectra (unpolarized) for hibbingite in sample DU-16, 1084.8 m. Lower spectrum: relatively unoxidized grain, showing the presence of Fe^{2+} (crystal field band around 12550 cm^{-1}). Top spectrum: oxidized grain, showing a $Fe^{2+} \rightarrow Fe^{3+}$ intervalence charge transfer band around 20000 cm^{-1} . The continuous increase in absorbance with increasing wavenumber in both spectra is due to diffusive scattering by imperfections in the crystal. Experimental conditions: 34- μm spot size, 30- μm sample thickness, 1000 scans, 4- cm^{-1} resolution, Xe arc lamp, Si detector, quartz beam splitter.

spectroscopy of Cl was used to compare hibbingite with hydrated and nonhydrated chlorides (Saini-Eidukat and Kucha, 1991). The $ClK\alpha$ emission peak position and the $ClK\beta/K\alpha$ ratio were found to be consistent with bonds involving OH groups as opposed to H_2O groups. The second method used the same Bruker IFS 120 HR spectrometer and IR microscope at the Bayerisches Geoinstitut to measure transmitted IR absorption spectra. Background was obtained through thin-section glass. To remove small features due to C-H and O-H stretching vibrations in epoxy, a spectrum from an olivine grain was also measured and subtracted from the sample spectra; this only resulted, however, in a very minor correction of the spectra. Figure 7 compares the spectrum collected from a hibbingite grain in sample DU-16, at 1084.8 m (top spectrum), with that of a grain from sample D-6A, at 560.0 m. Some small differences were observed (magnitude of small peak at approximately 3700 cm^{-1}), but in general the two spectra are quite similar to each other. The main peak at approximately 3552 cm^{-1} is typical for the O-H stretching vibration. The stretching vibration bands of OH^- measured for hibbingite agree with those measured for two other members of the chlorine hydroxide family, $\beta-Zn(OH)Cl$ and $Zn_5(OH)_8Cl_2$, in the range 3480–3600 cm^{-1} (Srivastava and Secco, 1967, as quoted in Farmer, 1974). The small peaks near 7000 cm^{-1} are overtones of the O-H stretching vibration. If H_2O molecules were present in the structure, a peak with wavenumbers in the region 5000–5200 cm^{-1} due to combined bending and stretching vibrations of H_2O would be present. The absence of such a peak indicates that only OH is present. The weak bands between 3900 and 4300 cm^{-1}

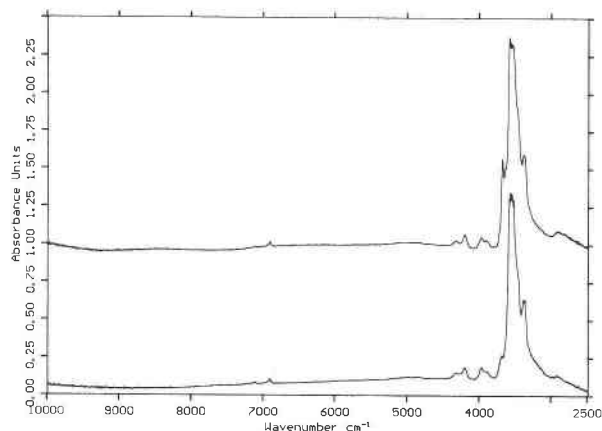


Fig. 7. Comparison of unpolarized IR absorption spectrum collected from a hibbingite grain in sample DU-16, 1084.8 m (top spectrum) with that of a grain from sample D-6A, 560.0 m (lower spectrum). Experimental conditions: 34- μm spot size, 30- μm sample thickness, 1000 scans, 4- cm^{-1} resolution, W source, narrow band MCT detector, Si-coated CaF_2 beam splitter. The strongest peak is centered at 3552 cm^{-1} . This peak is truncated because of the limited sensitivity of the MCT detector in this range. In reality, this band extends to much higher absorbances.

are due to combination modes of the O-H stretching fundamental mode with low-energy lattice vibrations (Farmer, 1974).

NOMENCLATURE AND IMPLICATIONS

Oswald and Feitknecht (1963) synthesized two forms of $\text{Fe}_2(\text{OH})_3\text{Cl}$, the α and β forms, both of which are hexagonal; orthorhombic hibbingite is designated $\gamma\text{-Fe}_2(\text{OH})_3\text{Cl}$. Hibbingite appears to be the Fe end-member of a solid-solution series with kempite (Laverat et al., 1973, and N. S. Rudashevsky, unpublished data).

The occurrence of hibbingite has implications for the roles of serpentinization processes, of sea-floor alteration by hydrothermal fluids, and of Cl-bearing solutions in the genesis of Pt-group element deposits (Dahlberg and Saini-Eidukat, 1991; Saini-Eidukat and Kucha, 1991); in addition, perhaps its occurrence has implications for any process involving the oxidation of a Fe^{2+} -bearing compound. An active role for Cl in serpentinization was debated by Rucklidge and Patterson (1977) and Miura et al. (1981). A possible reaction (Rucklidge and Patterson, 1977) is $4(\text{Mg}_{0.75}\text{Fe}_{0.25})_2\text{SiO}_4 + 5\text{H}_2\text{O} + \text{HCl} \rightarrow 2\text{Mg}_3\text{Si}_2\text{O}_5(\text{OH})_4 + \text{Fe}_2(\text{OH})_3\text{Cl}$.

Experimental basalt-alteration studies (Berndt et al., 1988; Seyfried et al., 1986) provided geochemical evidence for formation of a Cl-rich mineral in midocean-ridge hydrothermal systems. Cl concentrations in experimental fluids fluctuated significantly during alteration, in a manner consistent with fluctuations observed at ridge-crest hot springs. Decreases were ascribed to the formation of an Fe- and Cl-bearing mineral that was limited to

early-stage alteration (Berndt et al., 1988; Seyfried et al., 1986). This interpretation is consistent with the occurrences of hibbingite observed in the Duluth Complex; hibbingite is more abundant in partially serpentinized samples and tends to be replaced by magnetite or goethite in more serpentinized samples.

The Duluth Complex shows textural and geochemical evidence for the remobilization of Pt-group elements by Cl-bearing late- or postmagmatic fluids (Mogessie and Stumpfl, 1992; Ripley, 1990). In the samples investigated in this study, secondary magnetite or goethite appears in textural relations similar to hibbingite and can be recognized as pseudomorphs of it (Fig. 2). Iron oxides with similar textures from other partially serpentinized mafic rocks could be used as evidence of Cl-fluid involvement in serpentinization.

During terrestrial weathering of meteorites, $\text{Fe}_2(\text{OH})_3\text{Cl}$ (probably the β form) appears to be the first corrosion product to form and has been identified in the meteorites Jerslev, Odessa, Sardis, Toluca, Walker County, Carbo, Waverly, Willamete, and Yamato 791694 (Buchwald, 1989). It appears that only minute concentrations of Cl and H_2O need to be present to begin the corrosion process and that, upon alteration to ferric oxide or hydroxide, the Cl is freed to participate again in an oxidation reaction. V. F. Buchwald, in a personal communication, noted that he has identified $\text{Fe}_2(\text{OH})_3\text{Cl}$ on reinforced steel bars in a swimming pool construction. Other environments where Cl is in contact with Fe-bearing compounds, such as steel in brine, should be investigated for the presence of hibbingite or its polymorphs.

Visible and infrared spectral observations of the Martian surface (Bell et al., 1990) indicate the presence of ferric oxide or hydroxide minerals there. Their formation by acid-oxidative weathering of sulfide-bearing komatiitic lavas was discussed by Burns and Fisher (1990, 1993). Their formation by thermal alteration reactions was discussed by Bell et al. (1993). An alternate formation process could be the $\text{Fe}_2(\text{OH})_3\text{Cl}$ -aided oxidation of Fe^{2+} minerals, such as olivine or pyroxene, shown to be present in less altered regions of the Martian surface (Pinet and Chevrel, 1990). It is possible that the 0.4–0.8 wt% Cl present in Martian sediment (Arvidson et al., 1989) could form small amounts of hibbingite or its polymorphs, which would act as a catalyst for the oxidation process.

ACKNOWLEDGMENTS

This work would not have been possible without the support of the Minnesota Department of Natural Resources Drill Core Library in Hibbing, Minnesota, and the encouragement of E.H. Dahlberg. Financial support from a Fulbright grant (B.S.-E.), applied at the Institut für Geowissenschaften, Leoben, Austria, and from a grant to E.F. Stumpfl from the Jubilee Foundation of the Austrian National Bank (H.K.) is gratefully acknowledged. H. Mühlhans (Leoben) and K. Ettinger (Graz) are thanked for microprobe assistance, and M. Berndt and P. Weiblen are thanked for fruitful discussion. F. Seifert and T. Sharp made it possible for B.S.-E. to visit and make measurements at the Bayerisches Geoinstitut.

REFERENCES CITED

- Albee, A.L., and Chodos, A.A. (1970) Semiquantitative electron microprobe determination of $\text{Fe}^{2+}/\text{Fe}^{3+}$ and $\text{Mn}^{2+}/\text{Mn}^{3+}$ in oxides and silicates and its application to petrologic problems. *American Mineralogist*, 55, 491–501.
- Arvidson, R.E., Gooding, J.L., and Moore, H.J. (1989) The Martian surface as imaged, sampled, and analyzed by the Viking Landers. *Reviews of Geophysics*, 27, 39–60.
- Bell, J.F., III, McCord, T.B., and Owensby, P.D. (1990) Observational evidence of crystalline iron oxides on Mars. *Journal of Geophysical Research*, 95, 14447–14461.
- Bell, J.F., III, Morris, R.V., and Adams, J.B. (1993) Thermally altered palagonitic tephra: A spectral and process analog to the soil and dust of Mars. *Journal of Geophysical Research*, E98, 3373–3385.
- Berndt, M.E., Seyfried, W.E., Jr., and Cook, S.S. (1988) Trace element evidence for formation of a Cl-rich mineral in mid-ocean ridge hydrothermal systems (abs.). *Eos*, 69, T11C-03.
- Buchwald, V.F. (1989) Mineralogi og Reaktionsmodeller ved Korrosion of Jordfundne Jerngenstande (Meteoritter og Oldsager). In *Yearbook, Danish Metallurgical Society*, p. 41–72. Dansk Metallurgisk Selskabs, Lyngby, Denmark.
- Burns, R.G., and Fisher, D.S. (1990) Iron-sulfur mineralogy of Mars: Magmatic evolution and chemical weathering products. *Journal of Geophysical Research*, 95, 14415–14421.
- (1993) Rates of oxidative weathering on the surface of Mars. *Journal of Geophysical Research*, E98, 3365–3372.
- Dahlberg, E.H., and Saini-Eidukat, B. (1991) A chlorine-bearing phase in drill core of serpentinized troctolitic rocks of the Duluth Complex, Minnesota. *Canadian Mineralogist*, 29, 239–244.
- Farmer, V.C. (1974) The infrared spectra of minerals, 539 p. Mineralogical Society, London.
- Khomenko, V.M., Langer, K., Woodland, A.B., Andrut, M., and Vishnevsky, A.A. (1993) Optical absorption spectra of synthetic skiaigite ($\text{Fe}_3^+\text{Fe}_3^+\text{Si}_2\text{O}_{12}$) and natural Fe^{2+} , Fe^{3+} -bearing garnets. *Terra Abstracts*, suppl. 1 to *Terra Nova*, 5, 491.
- Kucha, H., Osuch, W., and Elsen, J. (1993) Calculation of cell parameters and refinement of crystal structure from electron diffraction patterns. In S. Gorozycza, W. Osuch, H. Szymanski, B. Garbarz, and A. Zielinska, Eds., *Eighth Conference on Electron Microscopy of Solid State*, p. 82–92, 20–23 April 1993, Wroclaw, Poland.
- Laverat, A.G., Martínez, O.G., Ruiz, J.C., and Ríos, E.G. (1973) Hydroxy salts. XII. Hydroxychlorides of iron (II), manganese (II) and other heavy cations. *Anales de Quimica*, 69, 331–337.
- Miura, Y., Rucklidge, J.C., and Nord, G.L., Jr. (1981) The occurrence of chlorine in serpentine minerals. *Contributions to Mineralogy and Petrology*, 76, 17–23.
- Mogessie, A.M., and Stumpfl, E.F. (1992) Platinum group element and stable isotope geochemistry of PGM-bearing troctolitic rocks of the Duluth Complex, Minnesota. *Australian Journal of Earth Sciences*, 39, 315–325.
- Oswald, H.R., and Feitknecht, W. (1963) Über die Hydroxidhalogenide $\text{Me}_2(\text{OH})\text{Cl}$, -Br, -J, zweiseitiger Metalle (Me = Mg, Ni, Co, Cu, Fe, Mn). *Helvetica Chimica Acta*, 47, 272–289.
- Palache, C., Berman, H., and Frondel, C. (1951) The system of mineralogy, vol. 2 (7th edition), p. 69–73. Wiley, New York.
- Pinet, P., and Chevrel, S. (1990) Spectral identification of geological units on the surface of Mars related to the presence of silicates from Earth-based near-infrared telescopic charge-coupled device imaging. *Journal of Geophysical Research*, 95, 14435–14446.
- Ripley, E.M. (1990) Platinum-group element geochemistry of Cu-Ni mineralization in the Basal Zone of the Babbitt Deposit, Duluth Complex, Minnesota. *Economic Geology*, 85, 830–841.
- Rossman, G.R. (1988) Optical spectroscopy. In *Mineralogical Society of America Reviews in Mineralogy*, 18, 207–254.
- Rucklidge, J.C., and Patterson, G.C. (1977) The role of chlorine in serpentinization. *Contributions to Mineralogy and Petrology*, 65, 39–44.
- Saini-Eidukat, B., and Kucha, H. (1991) An iron chloride hydroxide from the Duluth Complex, Minnesota with implications for metal mobility in hydrothermal systems. In M. Pagel and J.L. Leroy, Eds., *Source, transport and deposition of metals: Proceedings of the annual meeting of the Society for Geology Applied to Mineral Deposits*, p. 127–130. Balkema, Rotterdam, Germany.
- Seyfried, W.E., Jr., Berndt, M.E., and Janecky, D.R. (1986) Chloride depletions and enrichments in seafloor hydrothermal fluids: Constraints from experimental basalt alteration studies. *Geochimica et Cosmochimica Acta*, 50, 469–475.
- Springer, G. (1989) Chlorine-bearing and other uncommon minerals in the Strathcona Deep copper zone, Sudbury District, Ontario. *Canadian Mineralogist*, 27, 311–313.
- Srivastava, O., and Secco, E.A. (1967) Studies on metal hydroxy compounds. II. Infrared spectra of zinc derivatives $\epsilon\text{-Zn}(\text{OH})_2$, $\beta\text{-ZnOHCl}$, ZnOHF , $\text{Zn}_2(\text{OH})_2\text{Cl}_2$, $\text{Zn}_2(\text{OH})_2\text{Cl} \cdot \text{H}_2\text{O}$. *Canadian Journal of Chemistry*, 45, 585–589 (not seen; extracted from Farmer, *The Infrared Spectra of Minerals*, 1974).

MANUSCRIPT RECEIVED MAY 24, 1993

MANUSCRIPT ACCEPTED JANUARY 24, 1994